



SYSTEM IDENTIFICATION FOR BASE ISOLATED BUILDINGS

A. Paredes ⁽¹⁾, R. Boroschek ⁽²⁾, M. Orchard ⁽³⁾

⁽¹⁾ Department of Civil Engineering, Universidad de Chile, aparedes@ing.uchile.cl

⁽²⁾ Department of Civil Engineering, Universidad de Chile, rborosch@ing.uchile.cl

⁽³⁾ Department of Electrical Engineering, Universidad de Chile, morchard@ing.uchile.cl

Abstract

A procedure for nonlinear structural system identification for base isolated buildings is proposed herein. The study looks for an identification algorithm capable of addressing the nonlinear behavior of this type of systems to strong motion, thus helping to improve the accuracy on the response and dynamic properties estimation when undergoing different amplitude excitations.

A variety of relevant techniques developed in the literature are reviewed, including Power Spectral Density (PSD), Multivariate Output Space State Error with moving window (MOESP-MW), Recursive Prediction Error Method (RPEM), Bayesian processors (UKF) and Particle Filter methods (PF).

The effectiveness of each method is evaluated and compared through simulated data from a set of MIMO models, including Bouc-Wen and Bilinear hysteresis accounting for the nonlinear behavior of base isolation. Also time history acceleration recordings of more than 90 seismic events recorded on an instrumented isolated confined masonry four-story building, between 1993 and 2014, are used to perform identification.

Limitations of the algorithms and models, associated to an increasing complexity on the identification problem are discussed throughout the paper. Results indicate that Particle Filter provides a more complete and appropriate tool to deal with the identification process for a base isolated building, given their good performance on non-stationary state and parameter estimation.

Keywords: Nonlinear System Identification, Base Isolated Structure, Real Time Health Monitoring, Particle Filter, Bayesian estimation.



1. Introduction

System identification for base isolated buildings deals with the problem of determining the dynamic properties of structures showing localized nonlinear response under strong earthquake motions due to their isolators' behavior. A base isolated building consists on a system that can be separated in two parts: the *superstructure*, that is usually a conventional building with relative higher stiffness, supported on the *substructure* or *isolation system* which provides flexibility to the global structure, partially decoupling the superstructure response from the ground motion. This feature produces a predominant response on the first horizontal modal frequency and generates lower relative displacements between superstructure floors compared to a fixed base building.

For design purposes the isolation nonlinear behavior is typically represented by means of hysteretic models, like Bouc-Wen [1 - 3] and the Multi-linear hysteretic model, both considered on this research.

Many attempts have been performed using non-parametric frequency-domain identification techniques with nonlinear responses from systems as base isolated buildings, bridges and buckling restrained brace structures [4, 5]. Also, parametric subspace realization and least squares estimation algorithms have been applied in buildings with stiffness degradation, non-linear behavior and soil structure interaction [6, 7]. Estimations on mostly analytical hysteretic structural models using Bayesian filters methods have been performed [8 - 10]. An overview on other popular methods applied to this type of systems can be found in [11].

Chile provides a natural laboratory for studying the structural response due to its high seismic activity, including one of the recent strongest earthquakes on history, the February 27, 2010 in Maule with magnitude Mw 8.8. To take advantage of this characteristic, some structures have been instrumented to record their response and study their dynamic behavior, including an experimental base isolated 4 story low cost housing project and its conventional twin constructed in 1992, both located in Santiago.

This paper proposes procedures for base isolated building identification, reviewing a group of relevant techniques including non-parametric methods based on Fast Fourier Transform (FFT), Power Spectral Density (PSD), Multivariate Output Space State Error (MOESP), Recursive Prediction Error Method (RPEM), Bayesian processors (UKF) and Sequential Monte Carlo/Particle Filter methods (SMC/PF). The study focuses on the performance of each method. First, we present an analytical study in which all the techniques are applied using simulated data, obtained by numerical models developed in a structural analysis software. Base isolated 4-story tridimensional models with different seismic excitation levels are used for this purpose. Subsequently, a large number of time history acceleration data, corresponding to an existing base isolated structure, is used to test the identification procedures.

2. Identification Algorithms

A brief description on each identification technique studied is presented herein.

2.1 Fast Fourier Transform (FFT) – Power Spectral Density (PSD)

These two non-parametric identification algorithms [12, 13] are based on the analysis of the signal frequency content. We use peak peaking in order to find a predominant frequency of the system. For the purpose of this paper, this approach is used to obtain a first approximation of frequencies and modal shapes of the system, with the latter based on the estimation of the frequency response function (FRF) of each time-history acceleration response.

2.2 Multivariate Output Error State Space algorithm with moving window (MOESP-MW)

It consists on a parametric subspace identification method [14], which assumes a deterministic discrete linear state space representation for the system (Eq. 1 - 2), by means of Hankel matrices, aiming to find the eigenvalues and eigenvectors of \mathbf{A} and the \mathbf{C} matrix, which are related to the modal properties of the structure (frequencies, damping and mode shapes) of an assumed equivalent linear structure.



$$x_{k+1} = \mathbf{A} x_k + \mathbf{B} u_k \quad (1)$$

$$y_k = \mathbf{C} x_k + \mathbf{D} u_k \quad (2)$$

A model order determination and separation between structural and non-structural identified properties needs to be performed on each moving overlapped time window, by the application of stabilization diagrams, modal assurance criterion (MAC) and prior limit values accounting for admissible physical dynamic properties, estimated from stable poles [15]. In order to capture nonlinearities the response is split in consecutive time windows.

2.3 Recursive Prediction Error Method (RPEM)

This algorithm [16] estimate the parameter θ based on its previous value and the difference between the predicted output value $\hat{y}(t)$, given by a polynomial model representing the system, and the measured observation $y(t)$, subtraction that is weighted by a Kalman gain factor $K(t)$. It follows the general expression given by (Eq. 3)

$$\theta(t) = \theta(t - 1) + K(t)(y(t) - \hat{y}(t)) \quad (3)$$

The form of the gain factor depends on the chosen model and the estimation algorithm, which in this case consist in the forgetting factor λ algorithm, similar to the one studied by Safak [17]. This approach diminish the importance of old measurements exponentially such that an observation that is τ samples old carries a weight that is equal to λ^τ times the weight of the most recent observation. For tracking a time variant parameter (LTV) a value $\lambda < 1$ must be specified (typically values between 0.9 – 0.995 are suggested, depending on the sampling frequency), while a value of $\lambda = 1$ allows to track time invariant parameters (LTI).

Prediction error methods seek to minimize the total estimation error, which can be scalar or multivariate, using nonlinear iterative procedures like the Gauss-Newton algorithm.

Models differ depending on the polynomials included on the representation. The general form for the scalar case is the showed by Eq. (4). The autoregressive (AR) polynomial $A(q)$, is related to the system dynamic behavior and modal properties (frequencies f_j and damping β_j) by means of its roots, p_{Aj} , as it is showed by Eq. (5), while the rational polynomial $C(q)/D(q)$ includes the part that cannot be explained by past input-output data, coming from the noise model ($y(t) | e(t)$).

$$A(q)y(t) = \frac{B(q)}{F(q)}u(t - k) + \frac{C(q)}{D(q)}e(t) \quad (4)$$

$$\beta_j = \frac{\ln\left(\frac{1}{|p_{Aj}|}\right)}{\left[\arg(p_{Aj})^2 + \ln^2\left(\frac{1}{|p_{Aj}|}\right)\right]^{1/2}} \quad f_j = \frac{\ln\left(\frac{1}{|p_{Aj}|}\right)}{2\pi\beta_j T_s} \quad (5)$$

The objective is to estimate the polynomial coefficients from the chosen model, to get the discrete system properties from linear system theory expressions Eq. (5). The selection of a given model structure (i.e. selecting polynomial orders), is based on well-known and standard criteria (typically AIC, FPE and BIC), while model validation is performed by means of comparing the measured and predicted model response as well as applying some statistical tests.

2.4 Bayesian Filters (UKF) and Sequential Monte Carlo Methods (PF)

These group of recursive algorithms [18] consider a stochastic discrete state space representation for the system, including a perturbation term modelled as a stochastic process in both transition and observation equations. It assumes a random variable state X with a sought probability density function (pdf), $p(X)$, based on the observed system response data Y .

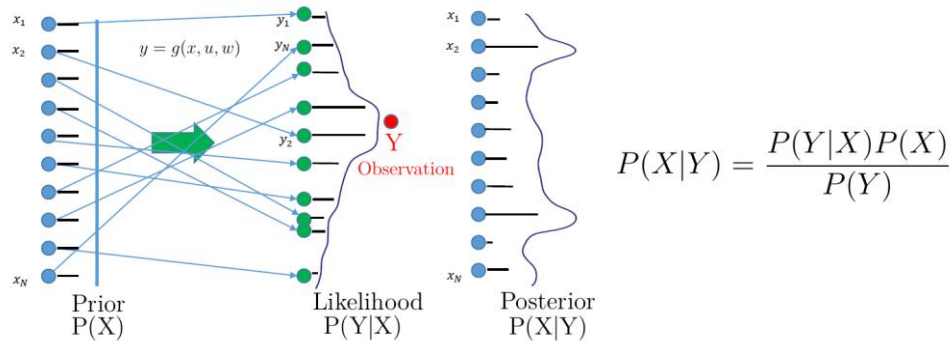


Fig. 1 – PDF Bayesian Filtering Estimation

The joint estimation (i.e. state and parameter) is made in two steps: 1) the prediction of the observation based on the internal states of the model, using the prior knowledge about them, $p(X)$, and 2) an update of the sought state/parameter taking into account the measurement, filtering the prior and getting a posterior distribution $p(X|Y)$ that accounts for the observed data (Fig.1). Depending on the model complexity is necessary to consider some constraints in the system to make the estimation problem numerically feasible, arising algorithms as the Kalman filter and approximate methods as the Extended Kalman Filter (EKF) and the Unscented Kalman Filter (UKF), with the latter having the capability to deal with nonlinear non-differential process and observation expressions using sigma points, which are defined by [19], to represent a Gaussian distribution.

On the other hand, Particle Filters – or SMC – algorithms aims to estimate an arbitrary form for the sought pdf, considering particles (i.e. state's values) with assigned weights, by Importance Sampling Techniques, assuming a known transition distribution $p(x_{k+1}|x_k)$. This approach is more convenient while the problem nonlinearity increases in a way that the Gaussian distribution it's not sufficient to represent an arbitrary distribution, but it requires larger computational cost than the previous methods.

3. Part 1: Analytical Study

3.1 Numeric Models

A 10×8m in plan base isolated 3D 4-story model constructed by a numerical software is used to get simulated acceleration responses to external seismic excitation, including some filtered white noise. Link elements with non-degrading hysteretic Bouc-Wen and multi linear plastic properties are used to represent the isolation characteristics (Fig.2). A total weight of 160 [Tonf] equally divided on each floor deck is assigned in the model. The isolation, material and geometric properties were chosen to match a value of 2.48 Hz and 2.78 Hz for the 1st mode frequency in Y and X directions respectively, as well as a damping of 5% for each mode. A post yield stiffness of 5% of the initial link stiffness was assigned, and seven different values for the yield force F_y , between 0.04 and 10 [Tonf] were tested, in order to generate different hysteretic behaviors along with an increasing excitation amplitude.

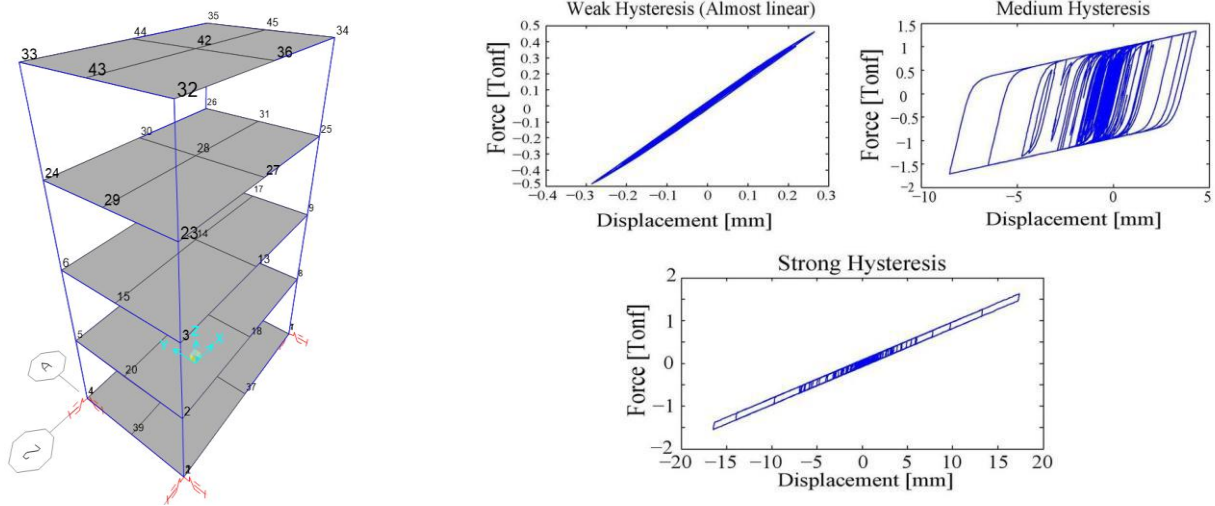


Fig. 2 – Numerical structure model and hysteretic cases for the analytical study

3.2 Results

3.2.1 - *FFT – PSD*: The model was subjected to increasing levels of white noise input. Nonlinearity increases with input excitation amplitude. The obtained Fourier spectrum does not indicate a clear consistent change in predominant frequency behavior as the hysteresis increases (Fig.3a). This procedure shows an identified frequency associated to a predominant stiffness in the hysteretic curve during the motion, which in this case doesn't present a smooth transition presumably because of the assumed non-degrading hysteretic models. This implies that even if the system exhibits a pronounced hysteretic behavior, the identified frequency could correspond to the one associated with the initial stiffness. A noticeable change occurs only for an extreme case with maximum displacements at the interface isolation level, higher than about 100 times the yield displacement u_y . These results were pointed out by Martinez et al. [5].

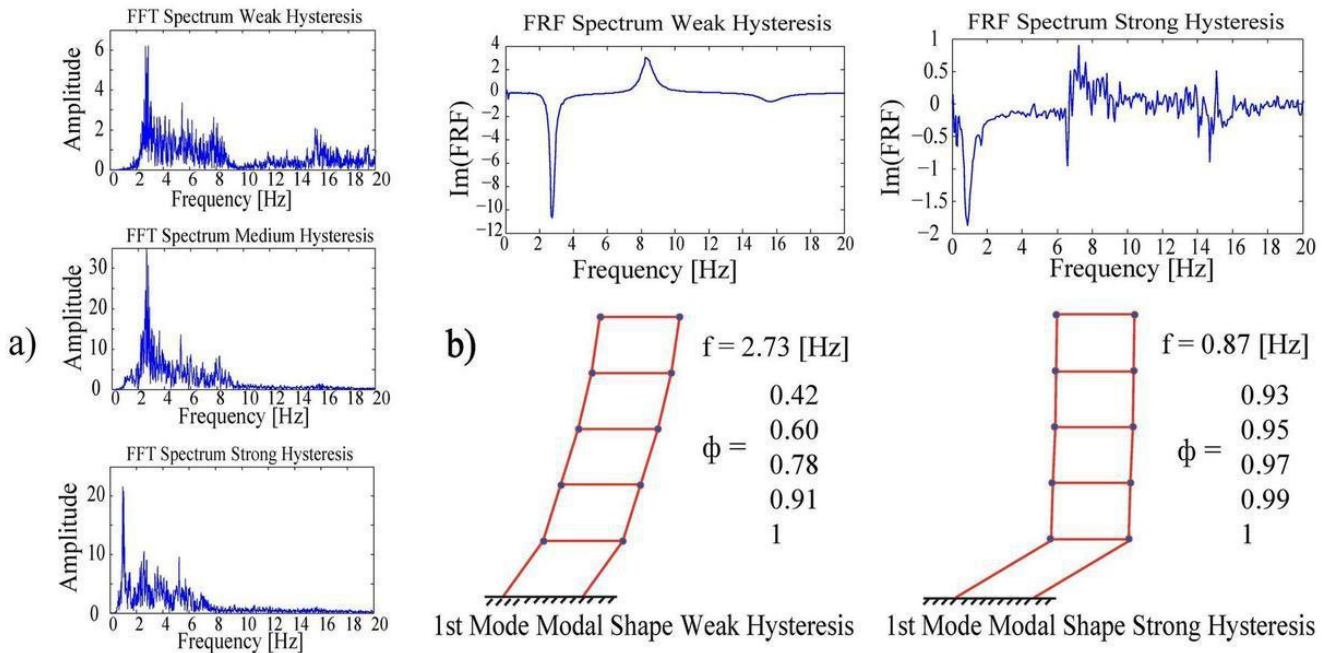


Fig. 3 – a) Change in FFT spectrum with hysteresis b) Change in FRF with hysteresis and 1st modal shapes

Besides the FRF shows a variable and irregular spectrum as the nonlinearity increases. The predominant frequency changes abruptly from the initial stiffness to the post yield stiffness. Modal shapes by this crude method are difficult to determine for higher modes (Fig.3b).

3.2.2 - *MOESP-MV*: Fig. 4 presents the variation of modal properties for a running window of length 1.5 - 3 sec. The 1st mode frequency values varies between 0.82 – 2.74 Hz for the X and 0.69 - 2.48 Hz for the Y direction, showing the dependence on excitation’s strength for different events. A histogram of the identified modal properties of each window is showed on the left of each pair of pictures corresponding to a specific excitation amplitude. It is seen that the stronger the motion is, the larger is the dispersion on the identified properties compared to the initial state in which the system behaves linearly elastic. Modal shapes are only coherent in the vertical direction, where the model’s behavior remains linear. Window time length selection must be made such it can identify transitions on the properties behavior, where a good value seems to be about 1.5 to 2 times the estimated longest period. Longer time windows tend to distort the identified values, reducing the ability of tracking the time-changing behavior of the parameters. Moreover, the number of records considered as well as their location have a strong effect on the identification accuracy, where the use of only a few of them results in a strong dispersion for all the identified modal properties.

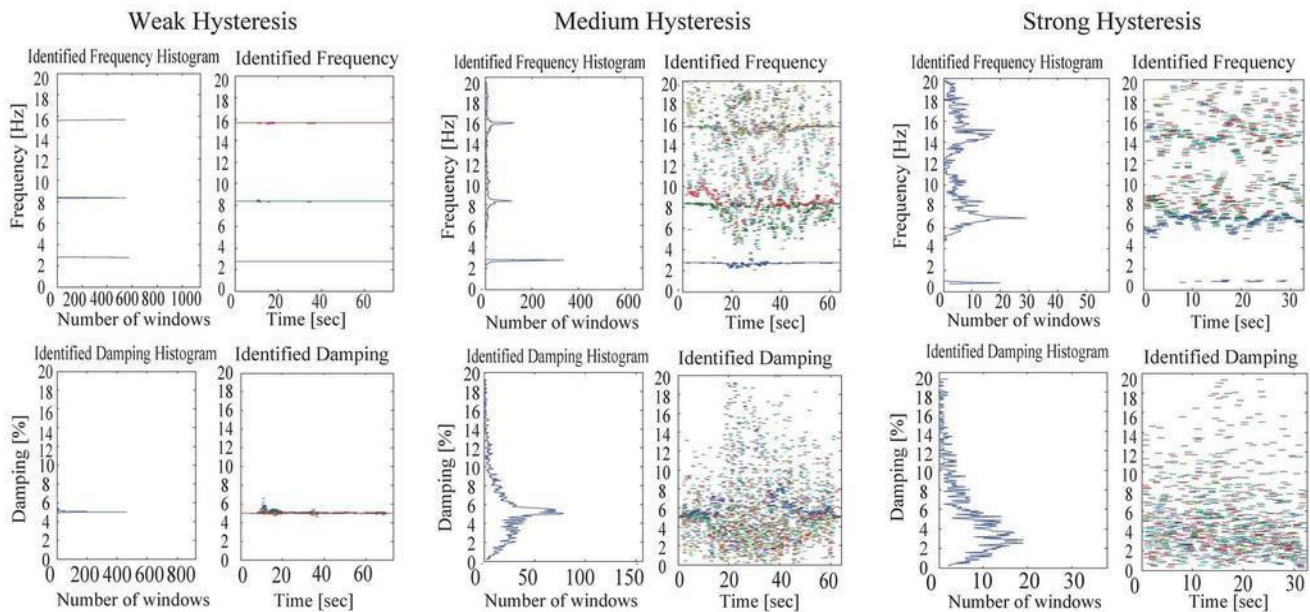


Fig. 4 – Identified frequencies and damping by MOESP-MW in X direction

3.2.3 - *RPEM*: For the application of this technique, an ARMAX ($F(q) = D(q) = 1$) model was selected by the minimum AIC, FPE and BIC value and then validated mainly by the comparison of the model predicted response and the actual measured output, following the guidelines in [20, 17]. Several values for the forgetting factor λ between 0.99 – 0.998 were tested, where the selection of an adequate factor is based on the sampling time, which in this case was $T_s = 0.005$ s. Fig. 5 presents the evolution of modal parameters for two levels of yielding strength. The results show that the identified properties depends strongly on the location of selected single channel measurement, with some of them being able to capture the variations for the horizontal 1st predominant frequency in the X direction, between 0.65 Hz and 2.78 Hz. For this mode, damping reaches values close to 100 %. For higher modes, identified modal frequency values remain similar compared to the elastic properties identified for smaller displacements, but with damping values bounded between 5 - 20%. Selection of proper initial values for the coefficients and covariance, seems to be very important to guarantee the convergence to the analytical properties. The selection of initial properties is done by an estimation considering a LTI model. The obtained results give that most of the tested models perform an adequate response estimation.

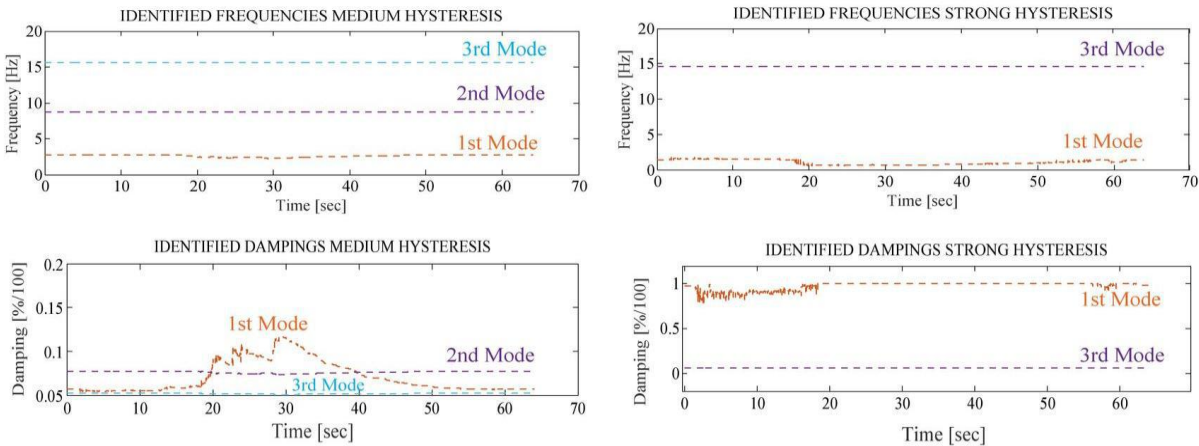


Fig. 5 – Identified frequencies and damping in X direction by RPEM for different hysteresis level

3.2.4 – UKF - PF: Several simplified state space representations addressing bilinear hysteretic models excited by white noise input, were tested using simulated responses generated by 4th-order Runge-Kutta integration. Selection of appropriate initial values and covariance are crucial for convergence to the right properties especially for UKF, given the system nonlinearity which generates multimodality on the sought parameter distributions. These are effectively estimated by Particle Filter. For testing these procedures, the next values for parameters to be estimated were assumed for a simple hysteretic model: $k_{isol} = 150$ [Kgf/m], $\alpha = 0.05$, $n = 0.8$ and $F_y = 50$ [Kgf]. Initial interval defined for tracking these parameters were $k_{isol} \in (1 - 500)$ [Kgf/m], $\alpha \in (0.01 - 0.9)$, $n \in (0.1 - 20)$ and $F_y \in (1 - 300)$ [Kgf]. A total number of 400 particles was use in order to estimate the posterior distribution of each sought parameter, assuming a Gaussian likelihood function for the innovation ($y_{obs} - y_{predic}$). Identified properties (Fig.6a) and predicted responses (Fig.6c) show good match with the ones corresponding to the numerical models when an adequate number of observations are available. Accurate estimates for hysteretic dynamic behavior, (Fig.6b), are achieved using acceleration response. However, incorporation of relative displacement as a measurement provides better convergence to the parameters characterizing the nonlinear response (stiffness ratio α and yield force F_y). This was pointed out by Chatzy, Xie and Li et al. [8- 10].

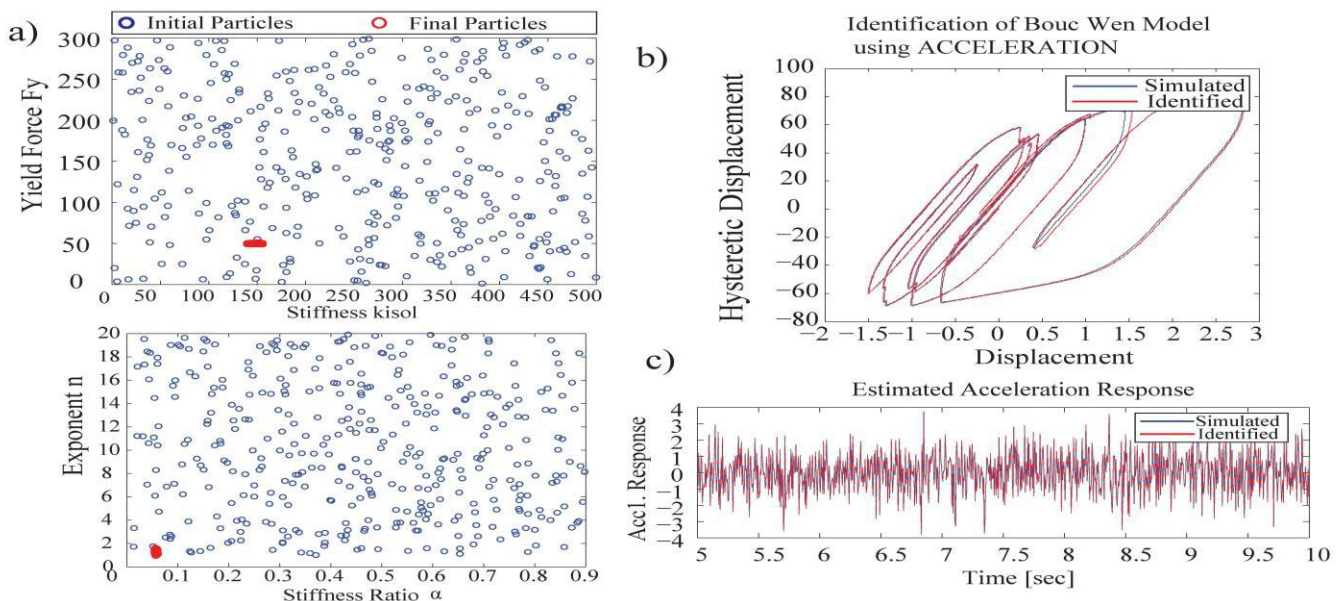


Fig. 6 – Identified dynamic properties a) Parameters Estimation by PF b) Hysteretic shape estimation using acceleration as observation c) System response estimation

4. Part 2: Identification with existing base isolated building

4.1 Outline of Building

The based isolated building used for this study consist in a 4-story low cost housing project, supported on eight high damping rubber isolators, constructed in Santiago, Chile in 1992 [22]. It's been instrumented with a local network of digital accelerometers that has recorded more than 90 seismic events between 1993 and 2014, including a major earthquake taking place on February 27, 2010 with magnitude Mw 8.8. The first floor is composed of reinforced concrete and the upper three of confined masonry. All floors have a 10 cm thick reinforced concrete slab, with the wooden roof. The bearings, 31.5 cm in diameter and 32 cm high, were composed of 34 layers of 6.7 mm thick high damping rubber and 33.2 mm steel shims. The building is instrumented with 2 triaxial accelerometers, in the first (L) and fourth floor (C). The seismic excitation is measured by another accelerometer located in the foundation level (F), recording acceleration in E-W, N-S and Vertical directions (Fig.7). The records were preprocessed by bandpass filtering with cutoff frequencies of 0.25 Hz and 30 Hz.

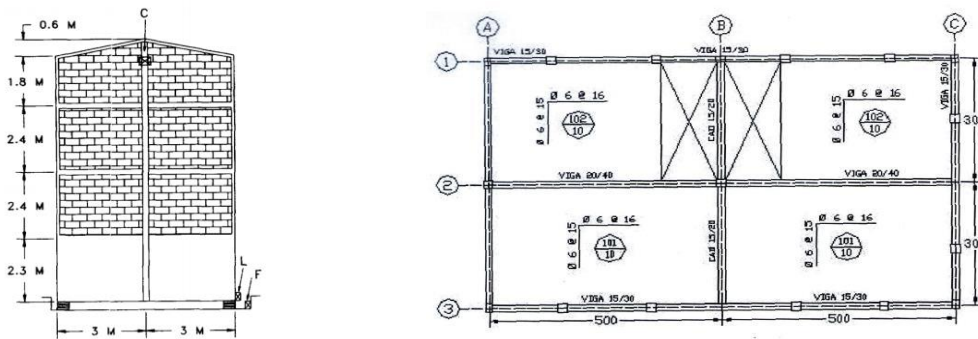


Fig. 7 – Accelerometer location and plan view of Comunidad Andalucía building [21]

4.2 Results

4.2.1 – FFT-PSD: Frequency spectrum shows two types of behavior depending on the relative displacement in the isolation. Identified predominant frequency values vary from 0.75 Hz to 5.59 Hz in the N-S direction, and 0.64 Hz to 6.07 Hz for the E-W direction for seismic events with a PGA ranging from 0.001 to 0.33 [g] and relative displacements 0.01 to 10.6 cm (Fig. 8a). The higher frequency values obtained for events with lower PGA agrees very well with some environmental vibration test performed previously on the building [22]. Unlike the analytical case, identified frequencies display a smoother transition with respect to displacement at the isolation interface level, because of the degrading and coupling behavior of the isolators, a characteristic that was not addressed on the analytical study. Vertical mode frequencies about 15-16 Hz for almost every seismic event are identified, showing that in this direction, the isolated structure remains almost linear. Identified modes (Fig.8b) are coupled, presenting a more significant contribution to the dynamic response of the structure on the indicated directions (**).

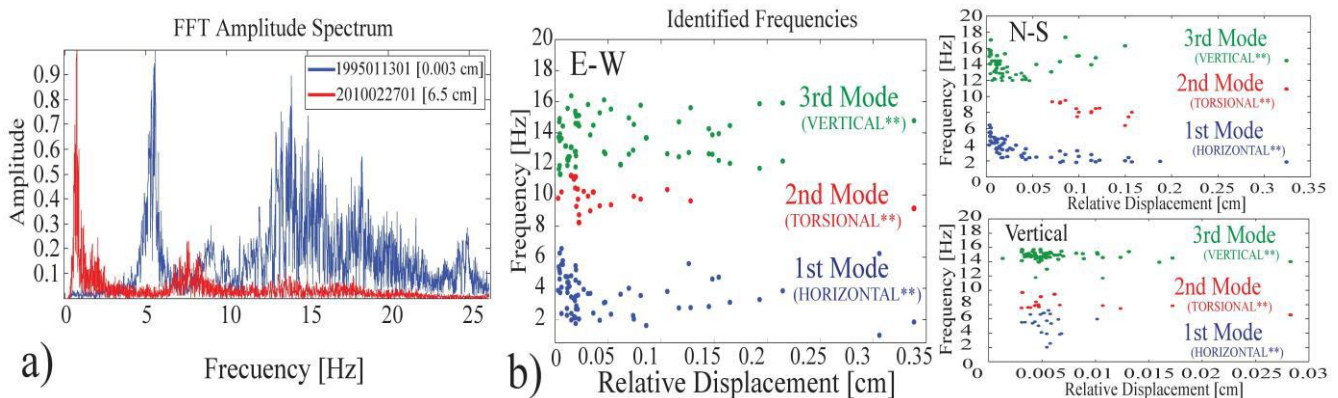


Fig. 8 – Identified properties by FFT in Comunidad Andalucía base isolated building: a) Normalized frequency spectrum for high (red) and small (blue) displacement. B) Frequencies v/s Relative Displacement in 3 directions.

4.2.2 – *MOESP-MV*: Values for 1st predominant frequencies ranges between 0.65 – 0.71 Hz for strong motion and 6.2 – 5.9 Hz for weaker excitation levels, using windows time length between 1.5 to 3 s (Fig.9). While vertical mode frequencies remain about 15 Hz for almost every excitation level, detecting mainly a linear behavior on this direction. As in the analytic study, damping presents great dispersion between consecutive identification intervals being just bounded for seismic events with lower excitation levels, showing a tendency to increase on the strong phase for these type of excitations, reaching values greater than 20 %, while in a weaker seismic excitation the damping is about 1 – 8 %. A consistent estimation on modal shapes was performed on the identification windows corresponding to the weak and strong phase of the earthquake motion for the 1st mode.

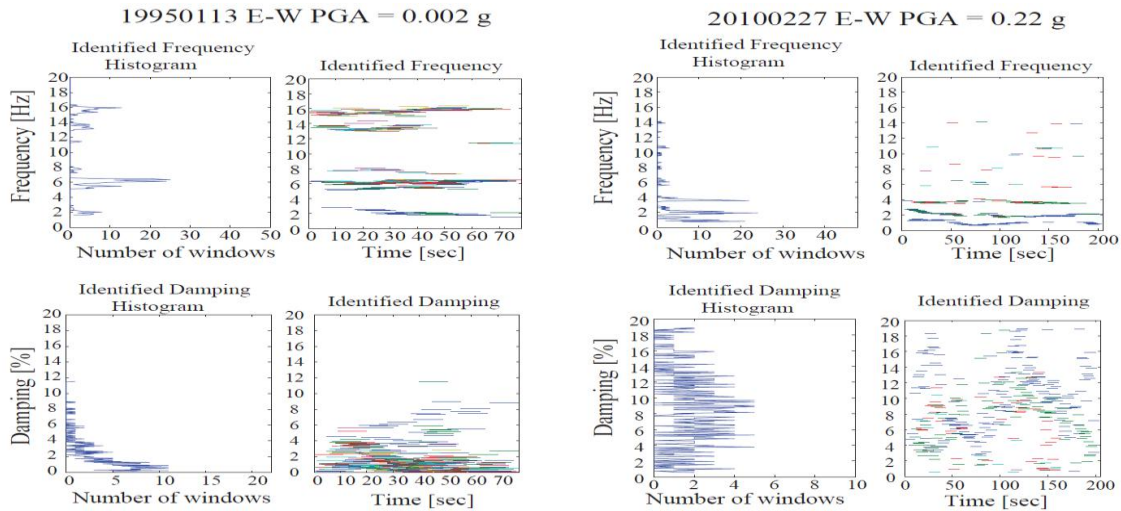


Fig. 9 – Identified frequencies by MOESP-MW in two events for Comunidad Andalucía building

4.2.3 – *RPEM*: Considering a forgetting factor $\lambda = 0.998$ ($T_v = 2.5$ s), horizontal modal frequencies varying between 1.04 Hz and about 6.1 Hz for E-W direction and between 1.18 Hz and 5.8 Hz for N-S directions were identified. Lower identified frequencies seem to be a bit higher than expected compared to the design value of the isolators. The algorithm shows a very stable response estimation, while the damping show an irregular behavior for the 1st horizontal predominant frequency, reaching values over 90 %. Damping for higher modes displays stable values between 10-20% (Fig.10b). Transfer functions (in this case represented by its FRF) generated by ARMAX model show variations of the 1st mode for 3 record time intervals, indicating that higher modes doesn't seem to be affected for the nonlinearity produced by the change of stiffness on the isolation system (Fig.10c). Tracking ability seems to be very good capturing the change in modal properties when strong phase of the motion takes place (Fig.10a). Most of the events characterize the structure as a model with polynomial order between $n_a = 16 - 24$.

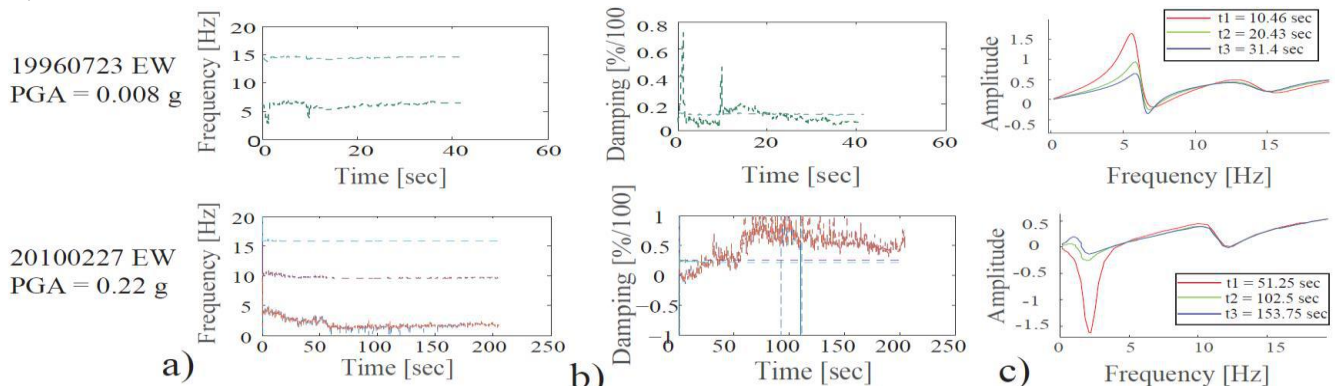


Fig. 10 – Identified properties for lower (up) and higher (down) PGA, by scalar approach of RPEM E-W direction: a) frequencies, b) damping and c) transfer function

4.2.4 – UKF – PF: Both methods were applied using simplified 1D models (M1, M2) in order to avoid non-observability problems due to the low number of sensors on the structure, depending on the number of available records for a given seismic event, showed in Fig.11a. The initial guesses for parameters of the superstructure (k_{str} , c_{str}) were adjusted based on a value between 9 Hz for E-W and 7.7 Hz for N-S direction, being an approximation to the first frequency mode observed from non-parametric techniques applied to data obtained by microtremors tests, and a damping value of 2%. While the admissible ranges for the isolation parameters were chosen as $n \in (0.1, 10)$, $\alpha \in (0.01, 0.9)$ and F_y , $k_{isol} > 0$ following Eq. (6-7) for the restoring force.

$$F(t) = \alpha \cdot k_{isol} \cdot u(t) + (1 - \alpha) \cdot F_y \cdot z(t) \quad \alpha = k_{yield}/k_{isol} \quad (6)$$

$$\dot{z}(t) = \frac{k_{isol}}{F_y} \dot{u}(t)(1 - |z(t)|^n) \quad (7)$$

The initial values were chosen based on the values estimated from experimental data [22]. As the uncertainty on the initial values is large, greater initial covariance (UKF)/particles spread (PF) are given to track the real properties ($\sigma_k = 10^3 - 10^4$ [Kgf], $\sigma_\alpha = 0.01 - 0.05$, $\sigma_{F_y} = 10^2 - 10^3$ [Kgf], $\sigma_n = 0.5 - 1$).

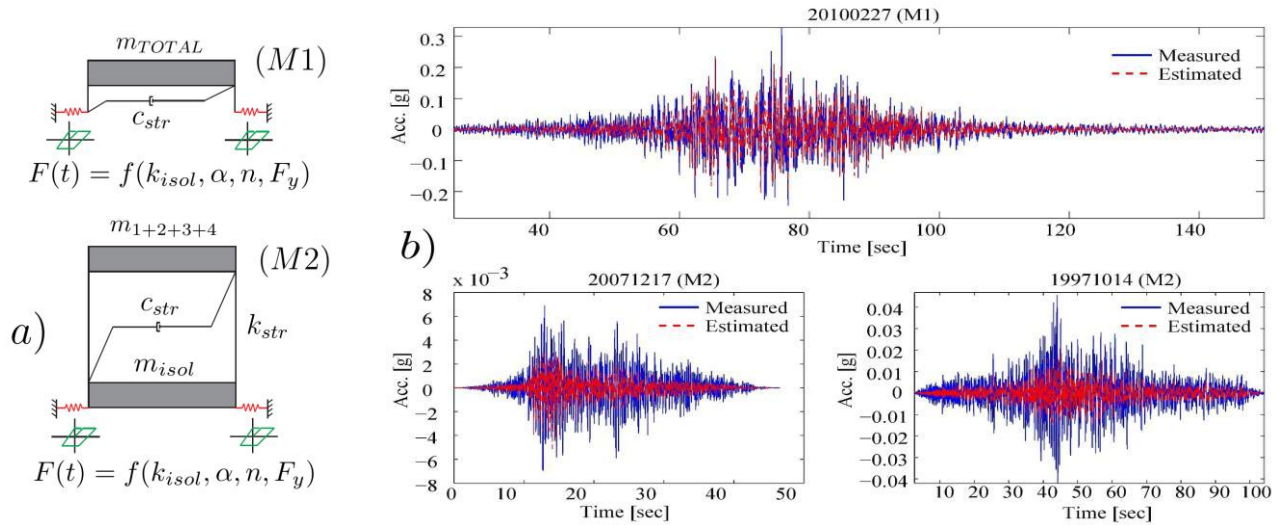


Fig. 11 – a) Simplified models of the structure b) Measured vs. Estimated 4th floor E-W accelerations by M1 and M2 for seismic events on Table 1.

The estimated structural parameters are compared with the equivalent values obtained from the pullback experimental tests performed in the building [23]. Even though these methods show fairly good response estimations (Fig.11b), maximum displacements are underestimated. This is explained by the oversimplified 1D model trying to address the general behavior of the existing isolated building based on the sought parameters. A few of the identified values using the database of seismic events are presented on Table 1. Close and consistent values are obtained for the initial stiffness of the isolation compared to the experimental one (obtained by static and dynamic tests) as the excitation is greater. Otherwise, events with small relative displacements (where the structure remains nearly linear) lead to varying values for n and F_y because of the absence of a developed hysteresis (although this tendency was also observed in strong excitation cases), but keeping a consistent value for the ratio of post-yield to pre-yield stiffness considering the observed behavior, where $\alpha \sim 0.8 - 1$ is obtained. Emphasis must be put on the selection of good initial values due to the variety of models that could approximate the measurements because of the number of parameters the model depends on (model non-observability problem) and also on the adequacy of the model used for the estimation. Despite of this, Particle Filter provides the different solutions representing the probability distribution of the sought parameters, so better results are expected while more prior information of the real structure is considered for the estimation.



Table 1 – Estimated parameters of the isolation model from Comunidad Andalucía building data

Direction	Event (ddmmyyyy)	Mw	PGA[g]	Model	Sensor Loc.	Max. disp.[cm]	Estimated max. disp. [cm]	k [Tonf/m]	Fy [Tonf]	η	α	$k_{exp[21]}$ [Tonf/m]	$\alpha_{exp[21]}$
E-W	14101997	6.8	0.019	M2	L, C	0.49	0.3	214.2	0.48	0.22	0.17	33 – 235	0.08 ^(*)
	17122007	5.4	0.004	M2	L, C	0.016	0.010	576.2	62.3	3.23	0.9		
	27022010	8.8	0.225	M1	C	6.51	3.81	183.4	0.83	0.18	0.23		

(*) Stiffness ratio estimated from fit experimental data.

5. Conclusions

An analytical and experimental study on 4 identification techniques applied to base isolated buildings has been presented. The results show that FFT/PSD, MOESP-MW and RPEM aim to identify nonlinear features of the system represented as varying linear properties, presenting strong limitations. Numeric models show that these methods tends to identify the predominant stiffness related frequency for different levels of response nonlinearities, presumably because of the assumed non-degrading hysteretic models. This implies that even if the system exhibits a pronounced hysteretic behavior, the identified frequency could correspond to the one related to the initial stiffness, limiting considerably the identification of nonlinearity (so for linear-based identification procedures purposes, bilinear models used here could not be sufficient to represent the real mechanisms that arise on hysteretic behaviors for the real isolation system). Determination of damping and modal shapes gets more difficult as increasing hysteretic levels are reached, being the latter consistent mainly for the first mode, and linear behavior as in the case of vertical direction.

The ability to track time-varying behavior using MOESP-MW is highly dependent on the selected time window and conditioned on the amplitude excitation due to the lack of consistency on identifying stable poles for the different phases of the earthquake. On the other hand, RPEM uses a single output approach, which limits the identified properties to the location of the measurement on the structure. However, these are able to detect frequency changes to seismic excitations, allowing to separate properties corresponding to the weak and strong phase of the building response, with values consistent with previous identified frequencies on the existing base isolated building, presenting a practical use for real time monitoring applications on these type of systems.

Model-based approach as UKF and Particle Filter show advantage on allowing to select a single model for different levels of excitations, characterizing in a more effective way the hysteretic behavior of the substructure and the almost linear behavior of the superstructure to an earthquake excitation. This does not occur for window linear methods. Nevertheless initial conditions for the parameters to be identified and complexity of the model selected are really important in order to get convergence to the right properties, being this selection more critical for the UKF given a supposed Gaussian distribution for the sought parameters, which are likely to be multimodal for this particular nonlinear model. Only in this case, the uniqueness of the model is still a problem that depends on the model observability, which Particle Filtering can overcome representing the real distribution as samples in high probability regions, including the sought solution, and characterizing the measurement noise through an appropriate likelihood function selection, leading to a good performance on estimation for structural properties and non-stationary states of the model.

Acknowledgements

The authors would like to thank Engineer Pedro Soto from Department of Civil Engineering University of Chile for providing the data and necessary information to develop the research.



References

- [1] Bouc, R. (1967). Forced vibration of mechanical systems with hysteresis. In *Proceedings of the fourth conference on non-linear oscillation, Prague, Czechoslovakia*.
- [2] Wen, Y.K. (1976). "Method for random vibration of hysteretic systems." *Journal of the engineering mechanics division* 102.2: 249-263.
- [3] Baber, T.T., and Wen, Y.K (1981). "Random vibration hysteretic, degrading systems." *Journal of the Engineering Mechanics Division* 107.6: 1069-1087.
- [4] Moroni, M., Sarrazin, M., Boroschek, R., Valdebenito, R., Romo, D. "Analysis of seismic records obtained in isolated structures", 12 World Conference on Earthquake Engineering, New Zealand, 2000, paper 1122.
- [5] J.M. Martínez, R. Boroschek, J. Bilbao. "System Identification procedures for nonlinear response of Buckling Restrained Braces". 7th International Conference on Structural Health Monitoring of Intelligent Infrastructure, SHMII, Torino, Italy, July 1st-3rd 2015.
- [6] Safak, E. (1989). Adaptive modeling, identification, and control of dynamic structural systems. II: applications. *Journal of engineering mechanics*, 115(11), 2406-2426.
- [7] Yoshimoto, R., Mita, A., & Okada, K. (2005). Damage detection of base-isolated buildings using multi-input multi-output subspace identification. *Earthquake engineering & structural dynamics*, 34(3), 307-324.
- [8] Chatzi, E. N., & Smyth, A. W. (2009). The unscented Kalman filter and particle filter methods for nonlinear structural system identification with non-collocated heterogeneous sensing. *Structural control and health monitoring*, 16(1), 99-123.
- [9] Xie, Z., & Feng, J. (2012). Real-time nonlinear structural system identification via iterated unscented Kalman filter. *Mechanical Systems and Signal Processing*, 28, 309-322.
- [10] Li, S. J., Yoshiyuki Suzuki, and M. Noori. "Identification of hysteretic systems with slip using bootstrap filter." *Mechanical Systems and Signal Processing* 18.4 (2004): 781-795.
- [11] Kerschen, G., Worden, K., Vakakis, A. F., & Golinval, J. C. (2006). Past, present and future of nonlinear system identification in structural dynamics. *Mechanical systems and signal processing*, 20(3), 505-592.
- [12] Cooley, J. W., & Tukey, J. W. (1965). An algorithm for the machine calculation of complex Fourier series. *Mathematics of computation*, 19(90), 297-301.
- [13] Bendat, J. S., & Piersol, A. G. (2011). *Random data: analysis and measurement procedures* (Vol. 729). John Wiley & Sons.
- [14] Verhaegen, M., & Dewilde, P. (1992). Subspace model identification part 1. The output-error state-space model identification class of algorithms. *International journal of control*, 56(5), 1187-1210.
- [15] Bakir, P. G. (2011). Automation of the stabilization diagrams for subspace based system identification. *Expert Systems with Applications*, 38(12), 14390-14397.
- [16] Ljung, L. (1998). *System identification* (pp. 163-173). Birkhäuser Boston.
- [17] Safak, E. (1989). Adaptive modeling, identification, and control of dynamic structural systems. I: Theory. *Journal of Engineering Mechanics*, 115(11), 2386-2405.
- [18] Candy, J. V. (2011). *Bayesian signal processing: Classical, modern and particle filtering methods* (Vol. 54). John Wiley & Sons.
- [19] Julier, S. J., & Uhlmann, J. K. (1996). *A general method for approximating nonlinear transformations of probability distributions*. Technical report, Robotics Research Group, Department of Engineering Science, University of Oxford.
- [20] Safak, E. (1991). Identification of linear structures using discrete-time filters. *Journal of Structural Engineering*, 117(10), 3064-3085.
- [21] Moroni, M. O., Sarrazin, M., & Boroschek, R. (1998). Experiments on a base-isolated building in Santiago, Chile. *Engineering Structures*, 20(8), 720-725.
- [22] Boroschek R., Moroni, M., Sarrazin, M. (1994) "Dynamic response of a Chilean base isolated confined masonry buildings", Workshop: Use of natural rubber bearings for seismic isolation of structures, Jakarta, Indonesia.